Available online at www.sciencedirect.com
ScienceDirect
Applied Surface Science 253 (2006) 974–982
applied surface science
www.elsevier.com/locate/apsusc

Implication of the role of oxygen anions and oxygen vacancies for methanol decomposition over zirconia supported copper catalysts

Gui-Sheng Wu, Lu-Cun Wang, Yong-Mei Liu, Yong Cao *, Wei-Lin Dai, He-Yong He, Kang-Nian Fan *

Department of Chemistry & Shanghai Key Laboratory of Molecular Catalysis and Innovative Materials, Fudan University, Shanghai 200433, PR China

Received 2 December 2005; received in revised form 16 January 2006; accepted 23 January 2006
Available online 28 February 2006

Abstract

The interaction of methanol with Cu, monoclinic ZrO_2, and Cu/m-ZrO_2 catalysts has been investigated by temperature programmed desorption (TPD) and reaction (TPRS) with the aim of understanding the nature of the surface sites and the mechanism involved in methanol decomposition. A synergetic effect has been detected since the combination of copper and ZrO_2 significantly facilitates the methanol decomposition with the facile evolution of H_2 and CO species at much lower desorption temperature. In conjunction with DRIFTS and H_2-TPD measurements of the Cu/ZrO_2 sample reduced at elevated temperatures, methanol decomposition over Cu/ZrO_2 is suggested to occur primarily on ZrO_2 with the aid of the presence of oxygen anions and oxygen vacancies generated by species-spillover between copper and zirconia. The interface between copper and zirconia is also evidenced to be crucial to the decomposition of methanol, with the main role of metallic Cu being to provide sites for H_2 removal by efficiently recombining the hydrogen atoms formed during the dehydrogenation of species located on zirconia.

Keywords: Temperature programmed desorption (TPD); Methanol decomposition; Cu/ZrO_2; The reduction temperature; Anionic vacancies

1. Introduction

During the last decades, the steam reforming of methanol for H_2 production over alumina-supported Cu/ZnO catalysts has attracted enormous interest in the development of fuel cell powered devices, especially for mobile applications [1–4]. The methanol steam reforming process is virtually a composite process involving methanol decomposition, the reaction of methanol with water, and the water–gas shift reaction [5]. Recent kinetic studies by Amphlett and coworkers [5] have shown that in order to obtain an accurate understanding and modeling of the methanol steam reforming process, the inclusion of the kinetically important methanol decomposition process must be considered. A detailed understanding of this step is believed to be a prerequisite for the design and development of new improved catalyst systems that can ensure substantial methanol conversion and high H_2 selectivity, together with the lowest possible amount of CO [1,2,5].

In developing more suitable catalysts for methanol reforming, copper supported on ZrO_2 has attracted considerable attention owing to their high activity and enhanced stability compared to their conventional ZnO-supported counterparts [2,6]. The better performances of zirconia containing catalysts have been attributed to higher Cu surface area, better Cu dispersion, and improved reducibility of Cu as compared with Cu/ZnO/Al_2O_3 catalysts [2,6]. Regarding the essential nature of metallic copper for the catalytic production of hydrogen from methanol steam reforming, recent studies by Ressler and coworkers [7] have experimentally demonstrated that although a high specific copper surface area is a prerequisite for catalytic activity, it does not account for the observed activity changes alone without taking the particular microstructure of the active Cu particles into account.

On the other hand, a number of recent studies concerning the mechanism of methanol decomposition or methanol synthesis from CO_2 hydrogenation over zirconia containing copper catalysts have revealed that the ZrO_2 is also an active component of the catalyst [8–12]. It has been generally accepted that catalysts containing copper and ZrO_2 behave in a bifunctional manner, with copper and ZrO_2 playing comple-

* Corresponding authors. Tel.: +86 21 65643977; fax: +86 21 65642978.
E-mail address: knfan@fudan.edu.cn (K.-N. Fan).

0169-4332/$ – see front matter © 2006 Elsevier B.V. All rights reserved.
doi:10.1016/j.apsusc.2006.01.056

mentary but different roles in methanol synthesis reaction [8–12]. Bianchi et al. [13] proposed similar bifunctional roles of Cu/ZrO_2 catalysts during methanol decomposition, where zirconia provides adsorption sites for reaction intermediates and Cu is proposed to facilitate the transfer of hydrogen. In this regard, a recent in situ FTIR investigation by Fisher and Bell [14] further revealed the involvement of the bifunctional roles of copper and ZrO_2 in the methanol decomposition. In spite of such bifunctional roles of copper and ZrO_2 as illustrated for methanol decomposition, the influence of the intrinsic surface nature of ZrO_2 on the beneficial synergy between copper and zirconium components in the Cu/ZrO_2 catalyst systems is not yet well understood.

In the present work, the interaction of methanol with Cu, ZrO_2, and Cu/ZrO_2 catalysts has been investigated by temperature programmed desorption (TPD) and reaction (TPRS) with the aim of understanding the nature of the surface sites of the ZrO_2 support involved in methanol decomposition. Since ZrO_2 is known to possess oxygen anion, oxygen vacancies and hydroxyl [8–14], introduction of copper or reduction of catalyst at different temperature will lead to changes in the distribution of these active sites. Therefore, special attention is paid to clarify the dependence of methanol decomposition behavior over the active sites of ZrO_2. In addition, the different roles of copper and zirconia as well as the beneficial synergy between copper and zirconium entailed by the strong metal-support interaction are also discussed in detail.

2. Experimental

2.1. Sample preparation

In general, copper catalysts supported on monoclinic zirconia tend to show higher catalytic performance for methanol synthesis or methanol decomposition than their tetragonal or amorphous counterparts [15]. Accordingly, monoclinic zirconia with a high surface area (S_{BET} = 86 m^2/g) obtained by the forced hydrolysis method described by Jung and Bell [16] was employed in the present work herein. Briefly, 0.5 M solution of zirconyl chloride ($ZrOCl_2{\cdot}8H_2O$) was boiled under reflux at 373 K and 1 atm for 240 h, while maintaining the pH at 1.5. The obtained precipitate was washed with deionized water until free of Cl^- ions, followed by drying at 393 K overnight and calcined at 673 K for 4 h. Pure copper was prepared by decomposition of copper nitrate at 673 K. Cu/ZrO_2 was prepared by impregnation of the monoclinic ZrO_2 by 5 mol% $Cu(NO_3)_2$ solution which was further dried at 393 K overnight, and calcined at 623 K for 4 h. The Cu/ZrO_2 catalysts reduced at different temperature were designated as CuZrRT, where T is for reduction temperatures.

2.2. Temperature programmed desorption (TPD)

One hundred milligram sample was placed between two layers of the quartz sand of U-type quartz reactor for TPD studies. The adsorbent tubes containing 5A-molecular sieve was equipped before bubbler of methanol in order to remove the trace of water in carrier gas (He). The catalysts were reduced in a stream (40 ml/min) of diluted hydrogen (5 vol.% H_2 in Ar) at temperatures ranging from 573 to 1073 K for 2 h. After the temperature decreased to room temperature, the methanol vapor carried by stream of He (40 ml/min) was introduced into the reactor for 60 min ensuring a saturated adsorption of methanol on the surface of catalysts. Subsequently, the reactor was swept with pure He stream (40 ml/min) until disappearance of methanol signal in tail gas. Eventually, TPD was carried out in the stream of He (40 ml/min) from room temperature to 1023 K with the ramping rate of 15 K/min. The *m/e* signals of 2, 18, 28, 28, 30, 32, 44, 46, and 60 corresponds to H_2, H_2O, CO, CH_2O, CH_3OH, CO_2, CH_3OCH_3 and $HCOOCH_3$ were monitored with an on-line quadrupole mass spectrometer (QMS200, Balzers OmniStar), respectively.

2.3. Diffuse reflectance infrared fourier transform (DRIFT) spectroscopy

The diffuse reflectance infrared Fourier transform spectroscopy was performed using a Bruker Vector 22 instrument equipped with a DTGS detector and a KBr beam splitter [17]. The catalyst powder (20 mg) was placed in a diffuse reflectance high-temperature cell (Harrick Co.). Prior to the experiment, the sample was maintained at 393 K in the N_2 stream (40 ml/min) for 60 min in order to remove the physisorption water on the surface of catalysts. Subsequently, diluted hydrogen (5 vol.% H_2 in Ar) was introduced and the temperature of the diffuse reflectance cell was raised to the desired temperature, i.e., 423, 573 and 673 K, respectively. After maintaining at the settled temperatures for 2 h, the spectra were recorded. To achieve satisfactory signal to noise ratio, a resolution of 4 cm^{-1} was chosen and 120 scans were averaged. The spectra were presented after subtraction of the background spectrum of mirror.

2.4. Catalytic characterization

The nitrogen isotherms and subsequently the multipoint Brunauer–Emmett–Teller (BET) surface areas (S_{BET}) of the samples were determined by N_2 adsorption at 77 K in the Micromeritics TriStar 3000 apparatus, using a value of 0.164 nm^2 for the cross section of the nitrogen molecule. The surface of pure copper in the reduced catalyst was determined with the use of the reactive adsorption of N_2O at 363K according to the method described in [18]. X-ray photoelectron spectra (XPS) was recorded with Al Kα radiation as the excitation source ($h\nu$ = 1486.6 eV). The sample pressed into a self-supported disc was mounted on the sample plate. Then it was degassed in the pretreatment chamber at 383 K for 2 h in vacuo before being transferred into the analyzing chamber where the background pressure was lower than 2×10^{-9} Torr. All the binding energy (BE) values referenced to the C 1s peak of contaminant carbon at 284.6 eV with an uncertainty of ±0.2 eV. Before XPS test, the catalysts after reduction were protected in N_2 atmosphere, which was treated

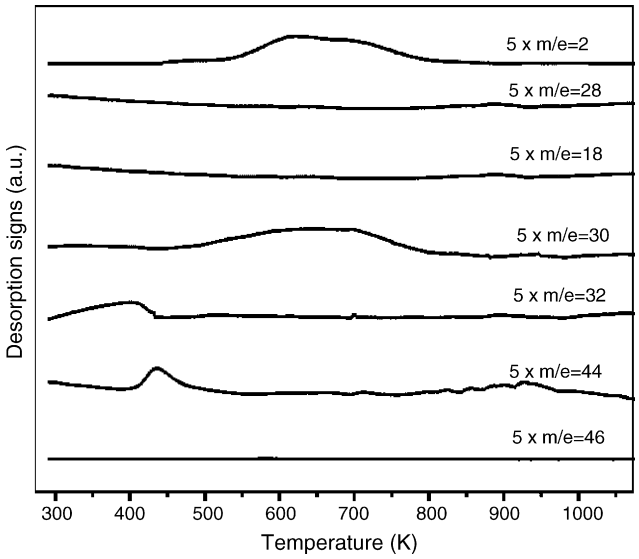

Fig. 1. TPD patterns of methanol on the surface of copper. *m/e* = 2, 18, 28, 30, 32, 44, 46, 60 corresponds to the desorbed species of H_2, H_2O, CO, CH_2O, CH_3OH, CO_2 CH_3OCH_3, $CHOOCH_3$, respectively.

by Ar ion sputtering in XPS process in order to remove the surface oxides induced by transitory exposition in air.

3. Results and discussion

3.1. TPD of Cu, ZrO_2 and Cu/ZrO_2

Methanol TPD profiles obtained from the pure polycrystalline copper are shown in Fig. 1. The desorption profile of *m/e* = 32 from room temperature to 423 K is attributed to the desorption of the physisorption methanol. The broad peaks of *m/e* = 30 in the range of 473–868 K are ascribed to the desorption of formaldehyde. It is well known that methanol on clean single-crystal Cu surfaces tends to show little or no reactivity. Previous studies concerning the interaction of methanol with single crystal copper surface revealed that only desorption of molecularly adsorbed methanol was observed on Cu(1 1 1) [19] and Cu(1 1 0) surface [20–22], and the presence of surface chemisorbed oxygen on the Cu crystal surface can significantly facilitate the adsorption of methanol [23,24]. In contrast, high-resolution XPS investigation indicated the dissociation of methanol into methoxy and formaldehyde occurred at around 200 K on Cu(1 1 0) before the entire desorption of all molecular species from the surface [25]. Recent methanol TPD studies on the Cu(2 1 0) surface also showed that half of the chemisorbed methanol decomposed into formaldehyde and H_2 at 100 K [26]. Analyzing the surface structure of copper employed in the above experiments, it is found that the interaction of methanol with the copper is structurally sensitive. It appears that the more closely packed the copper surface is, the less reactive is the dissociation of methanol. From the structural models of the Cu(1 1 1) and Cu(2 1 0) surfaces as shown in Fig. 2, it is seen that Cu(2 1 0) surface is more open than the Cu(1 1 1) surface. Additionally, the presence of step sites between the surface and subsurface or between the subsurface and the third layer can also be identified. All these differences can account for the more reactive properties of Cu(2 1 0). A number of theoretical studies also confirm that the metal atoms located at the open packed crystal surface, edge, corner, or step site are less index and show much more active properties [27]. In our case, the polycrystalline copper powder employed in the present work is believed to contain certain edges and corner sites which provide surface sites for partial decomposition of chemisorbed methanol into formaldehyde and H_2. In addition, the desorption of CO_2 at 431 K is also identified in Fig. 1. The oxygen for producing CO_2 might come from the incomplete reduced copper component or the trace of oxygen in the feed gas. Previous studies have evidenced the presence of oxygen species on the reduced Cu/$ZnAl_2O_4$ [28], Cu/ZnO/Al_2O_3 [29], and Cu/SiO_2 [30] catalysts is due to incomplete reduction. In addition, the trace amount of H_2O contained in the feed gas can be dissociated on the reduced polycrystalline Cu [31] to produce adsorbed oxygen and hydrogen. Although methyl formate was observed during the decomposition of methanol on Cu/SiO_2 [32], it was not detected in our experiments, possibly due to the intrinsically different properties of polycrystalline copper with respect to Cu/SiO_2. On the basis of the TPD patterns of all

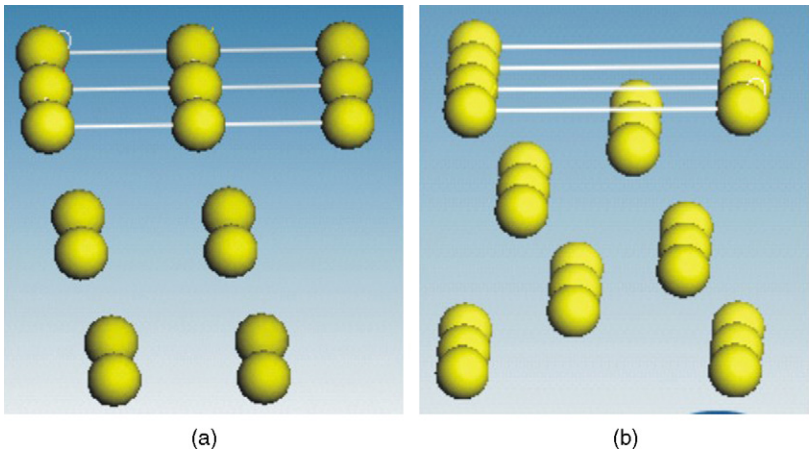

Fig. 2. The comparison of the model of Cu(1 1 1) (a) and Cu(2 1 0) (b) surface.

species, the methanol desorption and decomposition mechanism on the polycrystalline copper can be summarized as follows:

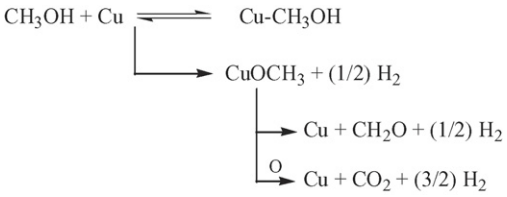

Note that methanol is mainly physisorbed on the surface of copper to produce adsorbed methanol which is unstable and can be desorbed easily. Furthermore, a small amount of methoxide is formed on the surface of copper, which either further decomposes into formaldehyde and H_2 or reacts with adsorbed oxygen to produce CO_2 and H_2.

The results of methanol desorption from pure zirconia (Fig. 3) show much stronger adsorption capacities for methanol with respect to pure polycrystalline copper. The broad peaks for signal $m/e = 32$ at 308–473 K and 473–789 K are related to the desorption of the physisorbed and chemisorbed methanol, respectively. For signals $m/e = 28$ and $m/e = 2$, the slight and strong desorption peaks at ca. 646 and 778 K are attributed to the surface evolution of CO and H_2 species. Notice that the main desorption of CO and H_2 needs a higher temperature than that of H_2O (at about 719 K). The IR results show that the surface of zirconia is covered by adsorbed water and hydroxyl (see the IR section), indicating that the released water in TPD process is due to the removal of adsorbed water and dehydration of vicinal hydroxyl on the surface of zirconia. Among them, the dehydration of vicinal hydroxyl (2-Zr–OH → –Zr–O^- + (–Zr)$^+$) can form oxygen anions and oxygen vacancies sites, which might be more crucial to the further decomposition of methoxide [31,32]. In addition, it is also identified that the desorption feature of dimethyl ether at 735 K is ascribed to the surface acidity of ZrO_2. Previous investigations of the adsorption of methanol on ZrO_2 or ZrO_2/SiO_2 by TPD and in situ IR methods have shown that at 323 K, gas-phase methanol can directly interact with hydroxyl groups of zirconia

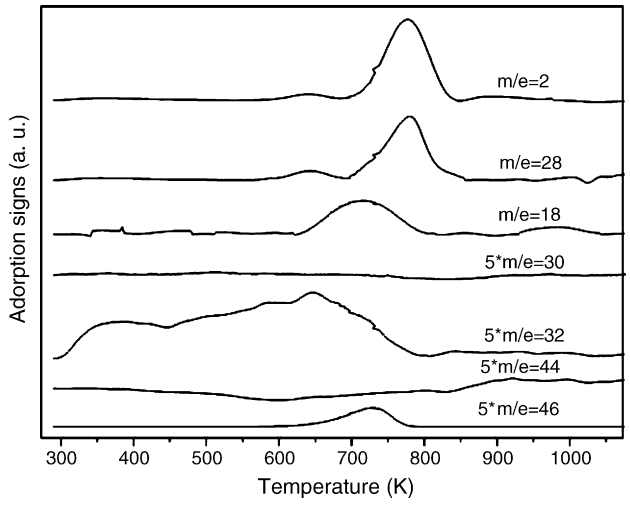

Fig. 3. TPD patterns of methanol on the surface of zirconia.

to form CH_3O–Zr and H_2O [33,34] or can interact with oxygen anions of zirconia to form methoxide and hydroxyl groups [14]. With increasing temperature, the predominant processes occurring are: CH_3O–Zr + H_2O → CH_3OH + HO–Zr, while the oxidation of CH_3O–Zr to b-HCOO–Zr at 523 K is an extremely slow process on ZrO_2/SiO_2 [14]. Compared with our results, there exists limited amount of oxygen anions and oxygen vacancies in the ZrO_2 or ZrO_2/SiO_2 mentioned above, because the adsorption and reaction temperature is not beyond 573 K. Our DRIFT and water TPD results display that the hydroxyl groups and adsorbed water on the surface of ZrO_2 are not well removed until 773 K. The surface hydroxyl and adsorbed water on the surface of zirconia might hinder the furthermore decomposition of methoxide into CO and H_2. With the increase of desorption temperature, the bridge hydroxyl and adsorbed H_2O on the surface of ZrO_2 are gradually consumed and more oxygen anions and oxygen vacancies are exposed, and then the decomposition of methoxide to CO and H_2 is promoted. The detailed scheme of methanol desorption and decomposition mechanism on the surface of zirconia is shown as follows:

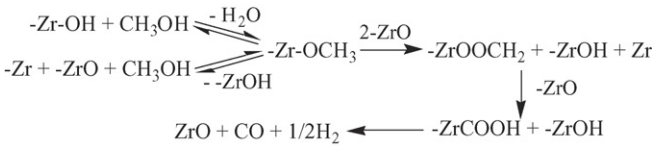

At first, methoxide can be formed on the surface of zirconia with the release of water when methanol interacts with surface hydroxyl or oxygen anions directly. With the absence of oxygen anions and oxygen vacancies, methoxide reacts with water to produce methanol and zirconium hydroxyl due to the slow decomposition process of the methoxide [14]. With the rise of the temperature, the surface hydroxyl and adsorbed water are removed, and then more and more surface oxygen anions and oxygen vacancies are exposed. The enrichment of oxygen anions facilitates the production of –$ZrOOCH_2$ through dehydrogenation of methoxide. With the aid of oxygen anions, –$ZrOOCH_2$ can decompose into –ZrOOCH, and then further into CO and H_2.

For the Cu/ZrO_2 catalysts (Fig. 4), the patterns of $m/e = 32$ at 374 K as well as at 536 K and 700 K correspond to the desorption of physisorbed and chemisorbed methanol, respectively. Desorption peaks of CO and H_2 are located at about 633 K with the tailed peaks at about 723–843 K. Compared with the methanol desorption action on the surface of pure zirconia, the main desorption peak at 633 K of Cu/ZrO_2 is in agreement with the weak desorption peak at 646 K. It is notable that the amount of desorbed water is low, indicating that there are lower surface hydroxyl and adsorbed water on Cu/ZrO_2, reduced at 573 K. This might be accounted for by the H and H_2O spillover from zirconia to copper, which can induce more oxygen anions and oxygen vacancies and then promote production of CO and H_2 at lower temperature. Although the H and adsorbed water spillover from zirconia to copper in the process of reduction is not reported in the previous literature, the spillover between copper and zirconia in the process of

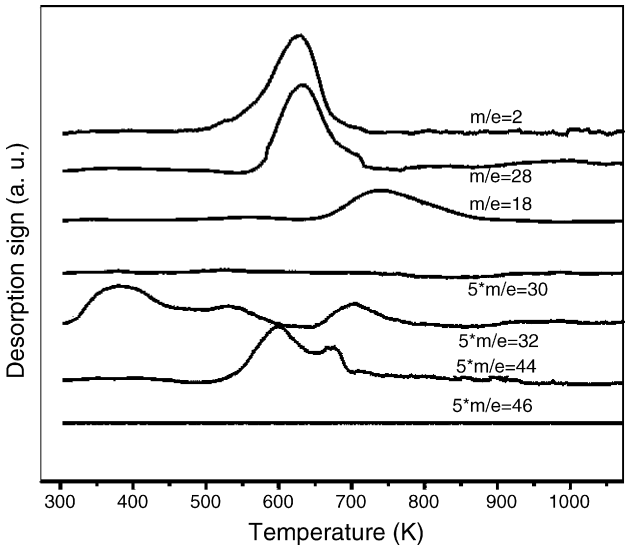

Fig. 4. TPD patterns of methanol on the surface of CuZrR300.

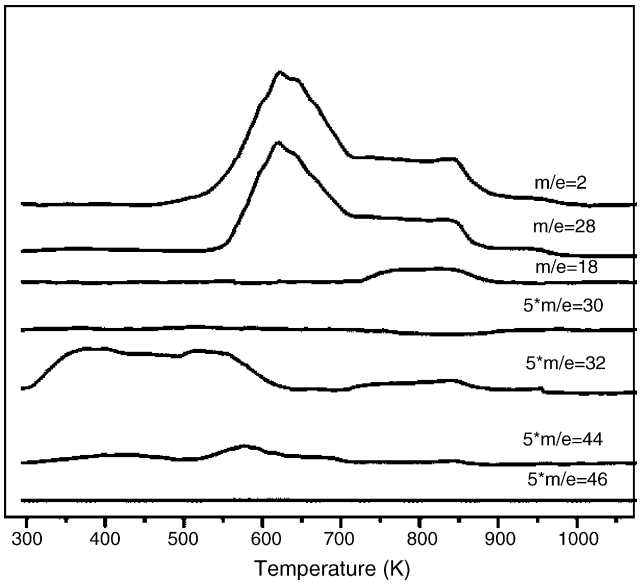

Fig. 5. TPD patterns of methanol on the surface of CuZrR550.

reaction is widely proposed by other authors. For example, Fisher and Bell [14] investigated methanol decomposition on Cu/SiO_2, ZrO_2/SiO_2, and $Cu/ZrO_2/SiO_2$ with IR methods. They suspected that the further decomposition of the methoxide groups on the surface of zirconia was promoted by the reverse spillover of hydrogen between copper and zirconia. For methanol synthesis from CO_2/H_2, it was also observed formation of b-HCOO–Zr and CH_3O–Zr at lower temperatures and at higher rates on $Cu/ZrO_2/SiO_2$ than on ZrO_2/SiO_2 owing to H spillover [35]. H spillover was imaged that the hydrogen required for these hydrogenation reactions to take place was supplied by spillover from Cu to the intermediates located on zirconia [36]. It is notable that the onset of H_2 desorption peak (478 K) are much lower than that of CO desorption peaks (558 K) in Cu/ZrO_2, indicating that H lose in the process of methanol decomposition is also promoted by induced H spillover between copper and zirconia. In addition, two desorption peaks of CO_2 at 596 and 675 K are also featured, which is much stronger than the pure copper.

3.2. TPD patterns of Cu/ZrO_2 reduced at different temperatures

On the basis of above discussion, the oxygen vacancies and oxygen anions on the surface of zirconia might be crucial to the methoxide decomposition. Furthermore, the species spillover between copper and zirconia not only influences the concentration of oxygen vacancies and oxygen anions, but also promotes dehydrogenation of adsorbed methoxide. Therefore, the interaction and the interface between copper and zirconia should play an important part in methoxide decomposition. It is practically convenient to change surface structure, surface composition as well as interaction among catalytic component by varying their reduced temperature [36,37]. It is well known that the reduction at high temperature can cause the envelopment of supporter about the active metal, and then the interface between metal and supporter changes remarkably [36]. In addition, the concentration of surface hydroxyl and adsorbed water will further decrease with the rise of reduced temperature. Therefore, methanol desorption on Cu/ZrO_2 reduced at the different temperature are investigated in the present work to enlighten the decomposition of methanol entailed to structure change.

TPD patterns of Cu/ZrO_2 reduced at 823 K (see Fig. 5) display the desorption peaks of CO and H_2 in the range of 573–673 K and in the range of 673–823 K. The desorption temperature in the range of 673–823 K is close to that in pure zirconia, inferring that the zirconium species are enriched on the surface of CuZrR823. Relative to the desorption of CuZrR573, a smaller amount of H_2O is desorbed, indicating that more adsorbed water or surface hydroxyl have lost and more oxygen vacancies and oxygen anions are formed. At about 581 K, it also displays the desorption peaks of CO_2, which is much weaker than in CuZrR573. This might be due to the increase of oxygen vacancies with the rise of reduction temperature.

For CuZrR1073 (see Fig. 6), only single desorption peaks of CO and H_2 are displayed at about 643 K, which is between the high- and low-temperature desorption peaks on ZrO_2. Because of no release of H_2O at the process of TPD, it indicates that the hydroxyl and the adsorbed water is well removed by reduction at 1073 K. Without the inhibition of surface hydroxyl, methoxide on the surface of zirconia can react with the Zr–O species to produce formate at lower temperature, which is further decomposed into CO and H_2. In addition, the reduction at 1073K might also envelop more zirconia on the surface of catalysts, which might lose the interface between copper and zirconia. Accordingly, the desorption temperatures of CO and H are higher than that in CuZr-573. Furthermore, it gives almost no evident desorption of CO_2, suggesting well removal of oxygen or formation of more oxygen vacancies by high temperature reduction.

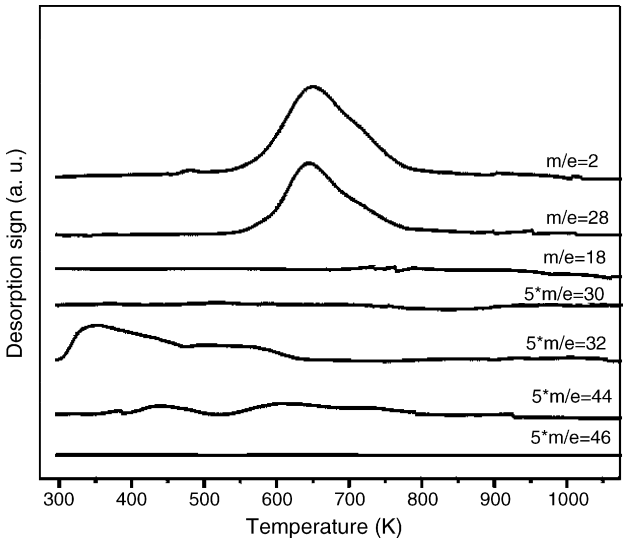

Fig. 6. TPD patterns of methanol on the surface of CuZrR800.

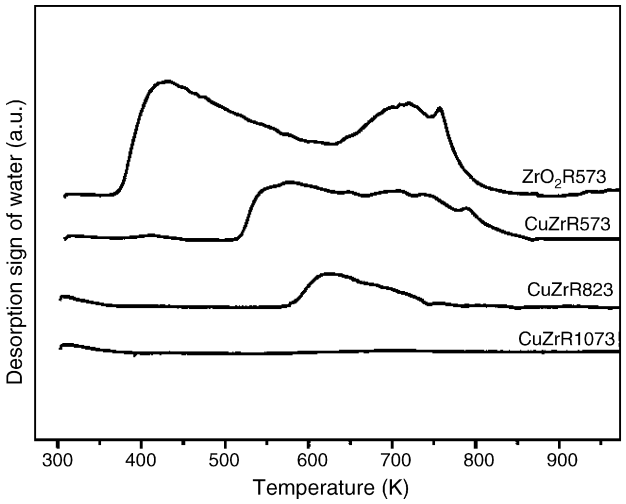

Fig. 7. Water desportion of Cu/ZrO_2 after reduction at different temperature.

3.3. H_2O desorption

In order to further elucidate the loss of water and surface hydroxyl with reduction temperature, Cu/ZrO_2 is reduced at different temperature at first, and then is employed to TPD study, in which desorption signs of water are recorded (Fig. 7). It is shown that CuZrR573 displays much less amount of desorbed water than zirconia reduced at 573 K, which further confirms the species spillover between copper and zirconia in the process of reduction. It is displayed much lower amount of desorption water in CuZrR823 and is not shown water desorption in CuZrR1023, illustrating more water and hydroxyl on the surface of zirconia are removed via the high temperature reduction. These results are in well agreement with the previous conclusion in methanol TPD.

3.4. The DRIFTS results

The hydroxyl changes on the surface of ZrO_2 and Cu/ZrO_2 with the reduction temperature are also monitored with DRIFTS to illustrate the types of hydroxyl on Cu/ZrO_2 and their change trends with reduction temperature (see Fig. 8). The two absorbed frequencies at 3640 and 3720 cm^{-1} are displayed in IR spectra of ZrO_2 and Cu/ZrO_2, which are attributed to the stretch vibration of bridged and terminal hydroxyl, respectively [34]. The broad absorbed peak ranged from 3800 to below 2500 cm^{-1} is ascribed to the adsorbed water [34]. With the rise of reduction temperature, the peaks due to the absorbability of bridged hydroxyl and adsorbed water decreases gradually on the surface of ZrO_2 and Cu/ZrO_2, while the hydroxyl at 3640 cm^{-1} decreases more rapidly in the Cu/ZrO_2 case. Furthermore, the peak area at 3640 cm^{-1} is fitted and is plotted as the reduction temperature (see Fig. 9). It also shows that the decreasing rate of 3640 cm^{-1} on the surface of Cu/ZrO_2 is about 1.5 times as that on the surface of ZrO_2. Previous study has evidences that the terminal hydroxyl is lost while the bridged hydroxyl changes slightly with adsorption of methanol [38]. Our results give the little change of terminal hydroxyl and evident loss of bridge hydroxyl with the rise of reduction temperature. This indicates that the rise of reduction temperature does not remarkably change the adsorbed sites of methanol. Loss of bridged hydroxyl might produce more oxygen anions and oxygen vacancies sites, which supply the sink of H for the adsorbed methanol or methoxide and promote the production of CO and H_2.

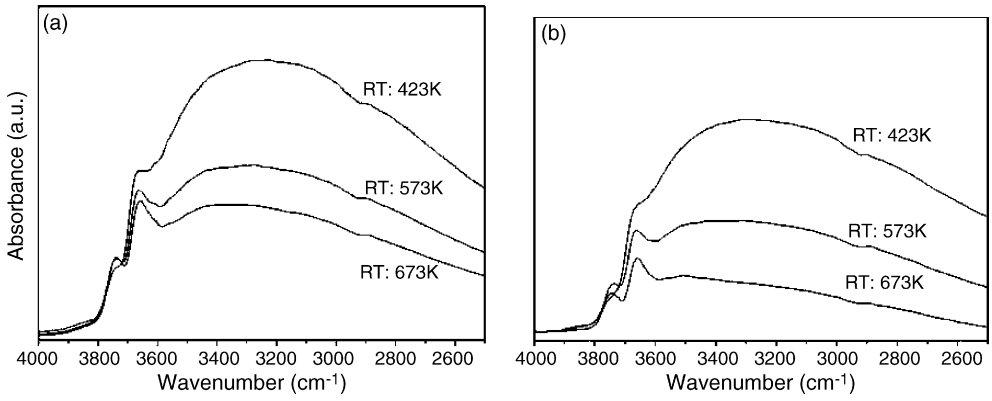

Fig. 8. The surface hydroxyl change of ZrO_2 (a) and Cu/ZrO_2 (b) with rise of reduction temperature.

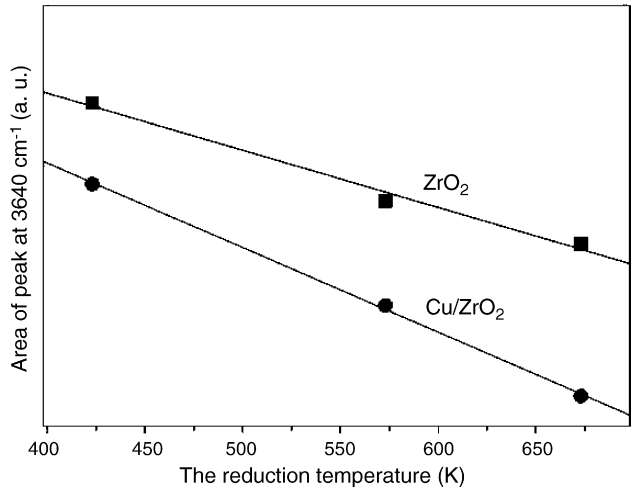

Fig. 9. The change of peak at 3640 cm^{-1} with the reduction temperature.

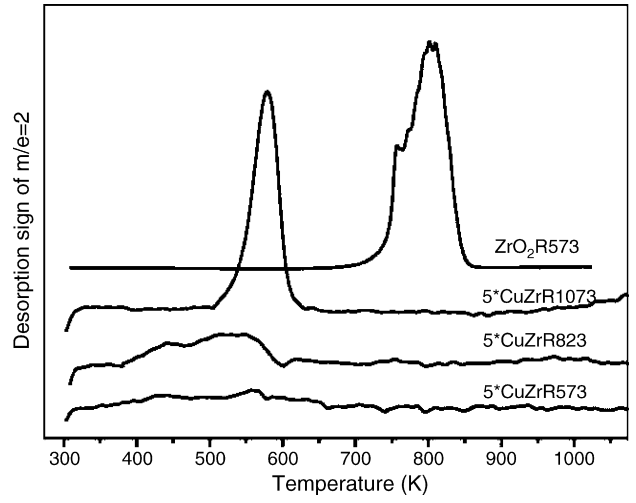

Fig. 10. H_2 TPD of catalysts reduced at different temperature.

3.5. H_2 TPD

The H_2 TPD results (Fig. 10) further evidence the reverse spillover effect of copper. It is shown that zirconia reduced at 573 K displays strong desorption peaks of H_2 at the range of 723–873 K, which is in agreement with the Bianchi's results [7–10]. But the CuZrR573 does not give evident desorption of H_2, which illustrates the copper species promote the loss of H_2 through H reverse spillover effect and then H_2 is well desorbed in the process of He sweep at low temperature. CuZrR823 displays evidence of H_2 signs, which becomes stronger on CuZrR1023. These results also illustrate that the more zirconia species spread on the surface of Cu/ZrO_2 with the rise of reduction temperature. Due to the spillover effect of copper, the desorption temperature of H_2 on CuZrR823 and CuZrR1023 is lower compare with those on ZrO_2.

Table 1
The surface element content of catalysts determined by XPS

Sample	Surface element content			S_{BET} (m^2/g)	S_{Cu} (m^2/g)
	O	Cu	Zr		
CuR300	–	–	–	0.3	0.2
ZrR300	82.04	0.00	17.96	86.0	–
CuZrR300	77.02	8.37	14.62	78.6	3.7
CuZrR550	74.83	8.44	16.73	73.8	3.0
CuZrR800	72.03	8.66	19.31	61.2	2.4

3.6. XPS results

In order to further specify the change of surface composition, Cu/ZrO_2 catalysts reduced at different temperatures are also investigated using XPS. From data of surface element in Table 1, it is illustrated that the content of surface oxygen decreases with reduction temperature, indicating of loss of adsorbed water and surface hydroxyl. These results are also in line with the conclusion of H_2O TPD and DRIFTS. Furthermore, the Zr content remarkably increases with the reduction temperature, indicating of the envelope phenomena of zirconia. In addition, the oxygen and zirconium species are also analyzed. According to the literature, there might be two types of O species in CuO/ZrO_2 after reduction, that is, O species of ZrO_2 or Cu_2O (O_I) and O species of Zr–OH (O_{II}), whose binding energy are about 531.5 and 532.5 eV [39,40]. Accordingly, the O 1s broad peaks are split into two peaks at the corresponding position using XPS peak-splitting program, whose relative content are shown in Table 2. It is shown that the content of O_{II} decreases with reduction temperature, further illustrating loss of surface hydroxyl. Similarly, the Zr $3d_{3/2}$ spectra is also split into two peaks at about 182.0 and 183.5 eV corresponding to Zr of ZrO_2 (Zr_I) and Zr of Zr–OH (Zr_{II}) species, respectively [40]. The relative Zr contents in Table 2 represent that the content of Zr_{II} also decreases with reduction temperature. Furthermore, the position of Zr_I shifts toward the lower binding energy, which might be contributed to be associated with the holes created by oxygen vacancies in the ZrO_2 lattice [39].

Table 2
The binding energies (eV) of Zr $3d_{5/2}$ and O 1s of catalysts

Catalyst	BE of Zr $3d_{5/2}$ (eV)		$Zr_{II}/(Zr_I + Zr_{II})$ (%)	BE of O 1s (eV)		$O_{II}/(O_I + O_{II})$ (%)
	Zr_I	Zr_{II}		O_I	O_{II}	
ZrR300	182.2	183.5	87.6	530.5	532.3	78.6
CuZrR300	182.1	183.5	53.6	530.5	532.2	49.4
CuZrR550	181.8	183.6	39.8	530.4	532.3	36.8
CuZrR800	181.5	183.4	12.3	530.4	532.3	11.2

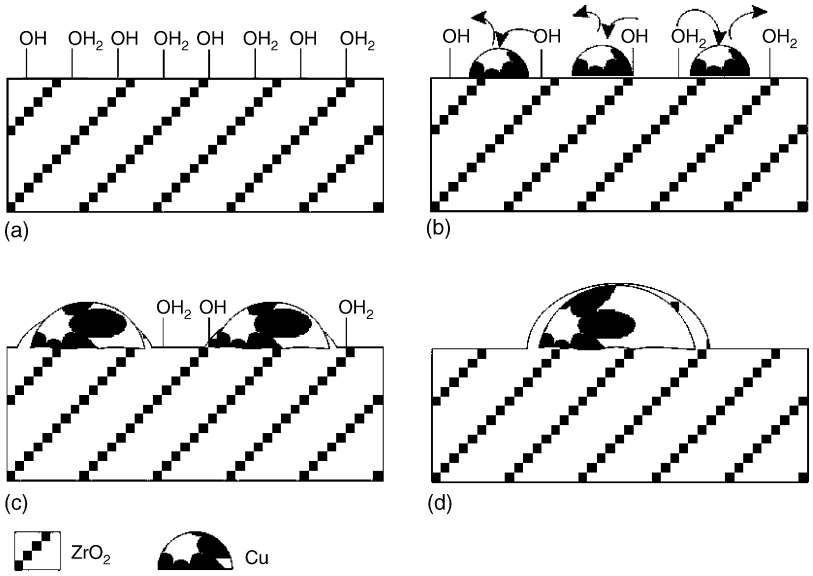

Fig. 11. The surface model of ZrO_2 (a) and Cu/Zr (b–d), from (b) to (d), the reduction temperature is increased.

The referee proposed if the differences of methanol adsorption capacity were due to the differences of the catalytic surface areas or the pure copper surface areas. The data of S_{BET} and the pure copper areas tabulated in Table 1 illustrated after the S_{BET} of CuZrR300 and ZrO2R300 are close, which cannot account for the remarkable difference of methanol desorption and decomposition. It can be conceived that the desorption intensity decreases with shrinkage of the catalytic surface because of decrease of adsorption sites. Although the S_{BET} and the surface area of pure copper decrease with the rise of reduction temperature, the desorption intensities in Figs. 4–6 do not show evident correlation with the surface area or the area of pure copper. Therefore, the adsorption difference on Cu/ZrO_2 reduced at different temperature should be ascribed to the change of active sites on the surface of catalysts.

From discussion above, it is concluded that methanol is more active on the site of zirconia, on which methoxide is formed at 323 K. However, the adsorbed methoxide is more difficult to further decompose because of surface hydroxyl and adsorbed water on the surface of zirconia. Above the desorption temperature at which the oxygen anions and oxygen vacancies are formed due to adsorption of water, adsorbed methoxide can be further decomposed into CO and H_2. Therefore, the oxygen anions and oxygen vacancies on the surface of zirconia might be crucial to methoxide decomposition. Methanol decomposition in Cu/ZrO_2 is promoted remarkably because copper component not only accelerates the formation of oxygen anions and oxygen vacancies by dehydration of hydroxyl and removal of adsorbed water, but promotes H transfer of methoxide adsorbed on zirconia to Cu. Accordingly, the interface between copper and zirconia is more important to methanol decomposition. The surface changes of zirconia with introduction of copper and increasing reduction temperature are modeled in Fig. 11. The surface of zirconia is featured by surface hydroxyl and adsorbed water (Fig. 11a). With introduction of copper, the oxygen anions and oxygen vacancies are easily formed because the H atom and adsorbed water spillover from zirconia to copper (Fig. 11b). With the rise of reduction temperature, zirconia and copper are aggregated which might be unfavorable to catalytic performance. However, parts of zirconia envelop on the copper particles and parts of hydroxyl and adsorbed water are removed (Fig. 11c). These changes can enlarge the interface between copper and zirconia and make more oxygen anions. Therefore the methanol decomposition is promoted. When reduction temperature is further increased, copper aggregated badly. Further, the large copper is well enveloped by zirconia (Fig. 11d). These cause the low activity of methanol decomposition because of loss of copper–zirconia interface.

4. Conclusions

In summary, pure Cu only shows the slight activity to the methanol adsorption, in which only physisorbed methanol or little amount of methoxide are formed. Methoxide can decompose into formaldehyde and H_2 or react with unreduced oxygen to produce CO_2. In contrast, zirconia shows strong adsorption capacity to methanol. The formed methoxide on the surface of zirconia can react with hydroxyl to produce methanol or decompose into CO and H_2 at higher desorption temperature. The concentration of oxygen anions and vacancies on the surface of zirconia might be crucial to the decomposition of methoxide. In the case of Cu/ZrO_2, release of CO and H_2 is observed at much lower desorption temperature owing to more oxygen anions and oxygen vacancies species on the surface Cu/ZrO_2. The results of IR and TPD of H_2 and H_2O further prove that copper can promote the loss of Zr–OH and adsorbed water, and then accelerates the formation of oxygen anions and vacancies. With the rise of reduction temperature, the activity of Cu/ZrO_2 changes due to the alteration of interface between zirconia and copper as well as the distribution of active sites on the surface of zirconia.

Acknowledgments

The financial supports from National Natural Science Foundation of China (Grant Nos. 20503005, 20473021, 20421303, 20407006), the National Key Basic Research Program (Grant No. 2003CB615807) and The Research Fund for the Doctoral Program of Higher Education (Grant No. 20050246071) are gratefully acknowledged.

References

[1] S. Hara, C. W-Xu, K. Sakaki, N. Itoh, Ind. Eng. Chem. Res. 34 (1999) 548.
[2] P.H. Matter, D.J. Braden, U.S. Ozkan, J. Catal. 223 (2004) 340.
[3] W. Cheng, Acc. Chem. Res. 32 (1999) 685.
[4] T.L. Reitz, P.L. Lee, K.F. Czaplewski, J.C. Lang, K.E. Popp, H.H. Kung, J. Catal. 199 (2001) 193.
[5] C.P. Thurgood, J.C. Amphlett, R.F. Mann, B.A. Peppley, Top. Catal. 22 (2003) 253.
[6] V. Ramaswamy, M. Bhagwat, D. Srinivas, A.V. Ramaswamy, Catal. Today 97 (2004) 63.
[7] H. Purnama, F. Girgsdies, T. Ressler, J.H. Schattka, R.A. Caruso, R. Schomäcker, R. Schlögl, Catal. Lett. 94 (2004) 61.
[8] D. Bianchi, T. Chafik, M. Khalfallah, S.J. Teichner, Appl. Catal. A 105 (1993) 223.
[9] D. Bianchi, T. Chafik, M. Khalfallah, S.J. Teichner, Appl. Catal. A 101 (1993) 297.
[10] D. Bianchi, T. Chafik, M. Khalfallah, S.J. Teichner, Appl. Catal. A 112 (1994) 57.
[11] D. Bianchi, T. Chafik, M. Khalfallah, S.J. Teichner, Appl. Catal. A 112 (1994) 219.
[12] Y. Sun, P.A. Sermon, J. Chem. Soc. Chem. Commun. (1993) 1242.
[13] D. Bianchi, T. Chafik, M. Khalfallah, S.J. Teichner, Appl. Catal. A 123 (1995) 89.
[14] I.A. Fisher, A.T. Bell, J. Catal. 184 (1999) 357.
[15] C. Morterra, G. Cerrato, F. Pinna, M. Signoretto, J. Catal. 157 (1995) 109.
[16] K.T. Jung, A.T. Bell, J. Mol. Catal. A 163 (2000) 27.
[17] Y. Cao, J.C. Hu, Z.S. Hong, J.F. Deng, K.N. Fans, Catal. Lett. 81 (2002) 107.
[18] J. Skrzypek, J. Słoczynski, S. Ledakowicz, Metanol Synthesis, Polish Scientific Publishers (PWN), Warszawa, 1994 , p. 45, and reference therein.
[19] J.N. Russell, S.M. Gates, J.T. Yates, Surf. Sci. 163 (1985) 516.
[20] M. Bowker, R.J. Madix, Surf. Sci. 95 (1980) 190.
[21] B.A. Sexton, A.E. Hughes, N.R. Avery, Surf. Sci. 155 (1985) 366.
[22] S.M. Francis, F.M. Leibsle, S. Haq, N. Xiang, M. Bowker, Surf. Sci. 315 (1994) 284.
[23] K. Varazo, F.W. Parsons, S. Ma, D.A. Chen, J. Phys. Chem. B 108 (2004) 18274.
[24] J. Greeley, M. Mavrikakis, J. Catal. 208 (2002) 291.
[25] C. Ammon, A. Bayer, G. Held, B. Richter, T. Schmidt, H.P. Steinruck, Surf. Sci. 507 (2002) 845.
[26] A.K. Chen, R. Masel, Surf. Sci. 343 (1995) 17.
[27] A. Ruban, B. Hammer, P. Stoltze, H.L. Skriver, J.K. Nørskov, J. Mol. Catal. A: Chem. 115 (1997) 421.
[28] C. Chauvin, J. Saussey, J.C. Lavalley, H. Idriss, J.P. Hindermann, A. Kiennemann, P. Chaumette, P. Courty, J. Catal. 121 (1990) 56.
[29] M. Bowker, R.A. Hadden, H. Houghton, J.N.K. Hyland, K.C. Waugh, J. Catal. 109 (1988) 263.
[30] G.J. Millar, C.H. Rochester, K.C. Waugh, J. Chem. Soc., Faraday Trans. 87 (1991) 2795.
[31] G.C. Chinchen, M.S. Spencer, K.C. Waugh, D.A. Whan, J. Chem. Soc., Faraday Trans. 183 (1987) 2193.
[32] M.Y. He, J.G. Ekerdt, J. Catal. 87 (1984) 381.
[33] A.M. Hussein, N. Sheppard, M.I. Zaki, R.B. Fahim, J. Chem. Soc. Faraday Trans. 87 (1991) 2655.
[34] T. Merle-Méjean, P. Barberis, S. Ben Othmane, F. Nardou, P.E. Quintard, J. Eur. Ceram. Soc. 18 (1998) 1579.
[35] I.A. Fisher, A.T. Bell, J. Catal. 172 (1997) 222.
[36] E.D. Batyrev, J.C. van den Heuvel, J. Beckers, W.P.A. Jansen, H.L. Castricum, J. Catal. 229 (2005) 136.
[37] G. Wu, Y. Sun, Y. Lia, H. Jiao, J. Mol. Struct. (Theochem) 626 (2003) 287.
[38] R.A. Koeppel, A. Baiker, C. Schild, A. Wokaun, Stud. Surf. Sci. Catal. 63 (1991) 59.
[39] M.K. Dongare, A.M. Dongare, V.B. Tare, E. Kemnitz, Solid State Ionics 455 (2002) 152–153.
[40] J.A. Navío, M.C. Hidalgo, G. Colón, S.G. Botta, M.I. Litter, Langmuir 17 (2001) 202.